Passive, Non-intrusive Assay of Depleted Uranium

H. M. O. Parker[a], J. S. Beaumont[b], M. J. Joyce[a]

[a] *The Department of Engineering, Lancaster University, LA1 4YW*
[b] *International Atomic Energy Agency, 1400 Vienna, Austria*

Abstract

The ability to detect neutrons from the spontaneous fission of ^{238}U in samples of depleted uranium with organic liquid scintillation detectors is presented. In this paper we introduce a small modular organic liquid scintillator detector array that can detect changes in mass of ^{238}U between 3.69 g and 14.46 g. To do this, 18-hour assays of various masses of 0.3% wt. of depleted uranium dioxide were assessed using four EJ-309 detectors, a mixed field analyser operated in pulse gradient analysis mode, and associated counting components. We observe a background-corrected fast neutron count sensitivity of $(2.0 \pm 0.3) \times 10^{-4}$ n g^{-1} s^{-1} per detector. This research demonstrates a proof of concept for depleted uranium quantity to be assessed passively on a non-intrusive basis via its spontaneous fission decay.

Keywords: Depleted uranium, neutron assay, passive, radiation detection, spontaneous fission

Highlights

- Passive assay of depleted uranium based on the spontaneous fission of ^{238}U is reported.
- Assessment is demonstrated over a range in mass of ^{238}U between 3.69 g and 14.46 g.
- A fast neutron count sensitivity of $(2.0 \pm 0.3) \times 10^{-4}$ n g^{-1} s^{-1} per detector is observed.

1. Introduction

Depleted uranium is a by-product of the isotopic enrichment of uranium. It is defined as having an isotopic abundance of ^{235}U (and trace levels of ^{234}U) that has been reduced, typically $< 0.2\%$ wt. ^{235}U, relative to that which occurs naturally at 0.72% wt. The vast majority of depleted uranium (99.977% wt.) is therefore ^{238}U. The reduced proportions of ^{234}U and ^{235}U in depleted uranium render it approximately half the specific radioactivity of natural uranium, at approximately 15 kBq per gram. Further, since this is mostly in the form of α decay and the emitted radiation is short-ranged, depleted uranium poses little external radiation hazard.

Internally, exposure to depleted uranium can occur via inhalation, ingestion, percutaneous absorption and dermal penetration, with inhalation being the most prominent pathway. The principal sites of uranium disposition in the body are the kidneys, liver and bone. Toxicologically,

Email address: h.parker@lancaster.ac.uk (H. M. O. Parker)

Isotope	SF yield (n s^{-1} g^{-1})	(α, n) yield in oxides (n s^{-1} g^{-1})	Mass percent in 0.3% wt. DUO_2
^{234}U	5.02×10^{-3}	3.0	0.0038
^{235}U	2.99×10^{-3}	7.1×10^{-4}	0.3
^{238}U	0.0136	8.3×10^{-5}	99.7

Table 1: Spontaneous fission (SF) and alpha-n (α, n) neutron contributions from common isotopes of uranium [6, chap. 11]. Indicative mass percentages are included for the depleted uranium dioxide (DUO_2) utilised for the work presented in this research.

depleted uranium is both a heavy metal and a radioactive substance, with the health effects being largely associated with its chemical toxicity rather than its radiological properties. Elemental uranium is an active metal which dissolves readily in hydrochloric and nitric acids. It is pyrophoric and, when finely divided, ignites spontaneously in air; such combustion typically yields UO_2 and U_3O_8, and the formation of some UO_3 is possible after weathering. A number of comprehensive reviews of its health effects have been made [1, 2, 3].

It is estimated that 1.5 million tonnes of depleted uranium is stockpiled throughout the world as a result of enrichment associated with the use of uranium in power production and nuclear weapons. Its uses are limited but include minor applications in radiation shielding (due to its significant density) and as counterweights in aircraft. A few hundred tonnes of depleted uranium has been used for military applications, particularly in the form of armour-piercing shells. Relatively little has been used for this purpose, compared to the quantity which remains stockpiled, but it is via this route that the majority of contamination of the natural environment has occurred in the form of dusts and stray shells buried in the ground [4]. Perhaps the most attractive use in the future is as the fertile material in fast-spectrum nuclear reactor systems, for which it constitutes a significant source of energy.

Whilst neither fissile nor significantly radioactive, the majority of the world's depleted uranium stockpile exists in the form of uranium hexafluoride (DUF_6) stored in cylinders, with around 1547 kg and 8500 kg of DU in a full 30B and 48Y cylinder, respectively [5]. It is in this form that it poses perhaps the greatest hazard due to its tendency to decompose in moist air to yield the toxic products uranyl fluoride and hydrogen fluoride. This necessitates that storage containers are inspected regularly for corrosion and damage.

Aside from α decay and γ-ray emissions, a small amount of spontaneous fission of ^{238}U is also observed, resulting in neutron emission at a rate of 0.0136 n g^{-1} s^{-1} [6, Table 11-1, p. 339]. As most nuclear reactor fuel contains relatively high proportions of ^{238}U, this could be a valuable property for the passive assay of nuclear materials, particularly those arising as by-products from the enrichment process. Table 1 presents neutron yield rates for both spontaneous fission (SF) and (α, n) reactions for the three most abundant isotopes of uranium, and mass percentages of 0.3% wt. depleted uranium, as used in this research.

The rate of spontaneous fission of ^{238}U is lower than that exploited in a number of isotopes of neighbouring elements for materials assay, particularly those of the even-numbered plutonium isotopes, and consequently it has received less focus in terms of radiation measurement research. However, given the ongoing requirement to ensure nuclear materials are accounted for [7], safeguarded [8, p. 36] and that this is accomplished with minimal risk to people carrying out the measurement [9], opportunities to assay nuclear material containing ^{238}U passively and non-intrusively should be investigated thoroughly [10].

Method	Constraints
Active neutron assay	This method involves the use of neutrons to stimulate fission in a sample, which can render the equipment required more sophisticated than for passive methods, particularly in terms of flexibility and portability. [13, Chapter 1.6, p. 8]
γ-ray spectrometry	γ rays are attenuated significantly by high-Z materials and therefore do not penetrate large samples. Corrections to the results from these measurements can be made to account for the loss as a result of attenuation but these often require a large amount of information about the equipment and set-up. [6, Chapter 7.3.2, p. 200]
Total γ-ray counting	As above, γ rays do not penetrate high-Z materials well. [11]
X-ray fluorescence (XRF)	Cannot discern between isotopes of the same element and so enrichment cannot be measured. [6, Chapter 10, p. 313]
Passive neutron coincidence counting	Coincidence counting at very low spontaneous fission rates takes a considerably longer time than singles counting. [6, Chapter 16, p. 457]

Table 2: A description of the constraints of a variety of techniques used to identify SNM and ^{235}U enrichment compared with a passive, singles fast neutron measurement.

In any given sample, the amount of ^{238}U present is inversely proportional to enrichment of ^{235}U, ignoring the trace levels of ^{234}U. It can be inferred then, that measuring ^{238}U can provide composition information of the level of enrichment of ^{235}U. The ability to measure ^{235}U enrichment is desirable across a variety of scenarios, such as in the monitoring of reprocessed uranium, uranium ores, tails and in forensic applications. A variety of methods are used at present, including γ-ray spectrometry [6, Chapter 7.3.2, p. 200], total γ-ray counting [11], X-ray fluorescence (XRF) [6, Chapter 10, p. 313], spectrophotometry [12] and active neutron coincidence counting [13, Chapter 1.6, p. 8]. In some situations a combination of these techniques is used to identify source materials, and particularly Special Nuclear Materials (SNM), i.e., plutonium and uranium enriched in ^{233}U or ^{235}U, and to determine isotopic composition. The possibility that fast neutrons arising from spontaneous fission might be used to identify and characterise a sample of material has a number of potential benefits. A description of the constraints of the methods listed above compared with single-fast neutron assay is given in Table 2.

Neutron emission rates can vary independently of enrichment, dependent upon both the elemental and isotopic composition of the uranium compound constituting the sample in question. The (α, n) reaction can play a significant role in this regard, particularly in the case of compounds containing low-Z elements such as oxygen and fluorine. Uranium dioxide (UO_2) exhibits a neutron emission rate that is approximately constant until enrichments of around 60% wt. ^{235}U. This is because, whilst the spontaneous fission neutron rate decreases due to the fall in the proportion of ^{238}U, the (α, n) rate increases due to the associated increase in ^{234}U with increasing enrich-

Enrichment (% wt.)	SF yield (n s^{-1} g^{-1})	SF %	(α, n) yield in oxides (n s^{-1} g^{-1})	(α, n) %	Total neutron emission rate (n s^{-1} g^{-1})
0.1977	0.0136	99.3	0.0001	0.7	0.0137
0.3000	0.0136	99.3	0.0001	0.7	0.0138
0.7108	0.0135	98.5	0.0002	1.5	0.0137
3.001	0.0132	94.3	0.0008	5.7	0.0140
18.15	0.0111	79.3	0.0029	20.7	0.0140
31.71	0.0093	66.9	0.0046	33.1	0.0139
57.38	0.0059	41.3	0.0084	58.7	0.0143
69.58	0.0042	28.4	0.0106	71.6	0.0148
97.65	0.0005	1.5	0.0318	98.5	0.0323

Table 3: Spontaneous Fission (SF) and alpha-n (α, n) neutron contributions across a range UO_2 enrichments, adapted from [6, p. 413-414].

ment and its associated α decay, until approximately 60% wt. ^{235}U. Beyond this level, the (α, n) component becomes dominant [6, Ch 14.2.2, p. 412] and hence the neutron emission rate begins to increase. Adapting data from [6, p. 413-414] of neutron emission rate versus enrichment, Table 3 can be produced, and plotted in Fig. 1.

To demonstrate the detection of neutrons from the spontaneous fission of depleted uranium dioxide (DUO_2), samples of a range of masses of 0.3% wt, DUO_2 have been assessed in this research by way of proof of concept. It was decided to vary mass rather than enrichment, due to the approximately constant neutron emission rate from UO_2 below 60% wt. ^{235}U enrichment, described earlier. This has been done to explore the conjecture that, if a significant difference in neutron counts from each of the samples can be discerned, then this method might also be applicable to measure enrichment in certain scenarios. The graph shown in [6, Fig 14.3, p. 415] illustrates how the specific neutron emission rate of a number of uranium and plutonium materials and compounds varies with ^{235}U enrichment. It depicts UF_6, UO_2F_6, PuO_2, and PuF_4 all exhibiting significant differences in neutron production rate across the range of enrichments plotted. The presence of these differences suggest that the proof of concept purported in this paper could be adapted for total-singles-neutron counting of other compunds, as part of a suite of measurements for SNM.

To date, neutrons from the spontaneous fission of ^{238}U have been detected using a limited number of methods, including track-etch detectors [14] and ^{3}He detectors [15, Ch 14, p. 518][16]. Track-etch detectors allow a user to identify that a neutron has passed through the detector material but give limited indication of the energy with which it passed. The detectors are chemically hazardous and the signals they produce require somewhat intrusive post-processing in order to gain a neutron count [17]. Perhaps the most prominent means of detection for neutrons are counters filled with ^{3}He gas or, alternatively boron trifluoride. These detectors usually require the thermalisation of the incident neutrons and consequently much of the spectroscopic information about the neutrons is lost. Gas-filled detectors are also often used in coincidence or multiplicity mode, i.e., to identify multiple neutrons associated with the same fission event. This technique

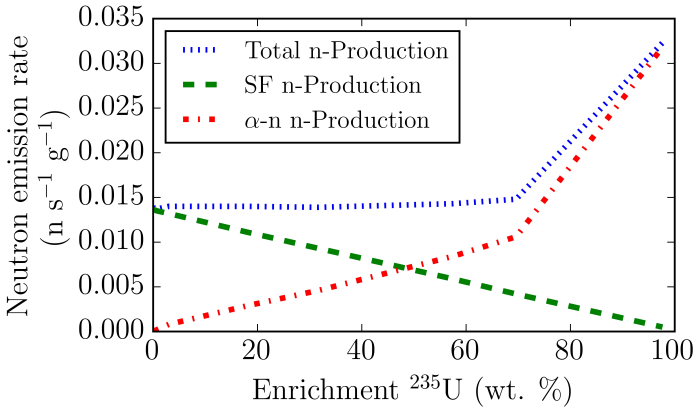

Figure 1: Neutron emission rates for uranium dioxide, adapted from [6, p. 413-414].

gives the user information on double and triple detection rates which can be used, for example, to infer the fissile mass of a given sample, and reduces the perturbation by neutrons that are not correlated directly with fission.

As touched upon in Table 2, detecting coincident neutron events usually increases the time necessary for an assessment in comparison to that based on the detection of single events. This is due to the reduction in efficiency of the system, for example the detection of two neutrons in coincidence is proportional to the square of the detector efficiency (ε^2). Further, ^{3}He is supply-constrained and, as it has become less widely available, its cost has increased and alternatives have been sought. Boron trifluoride, whilst a substitute, is potentially hazardous were it to leak and be inhaled.

The use of organic liquid scintillator detectors provides a number of benefits over the two approaches summarised above. The interaction mechanism between the liquid scintillation material and an incoming neutron affords spectral information about the sample [18]. Fast neutrons are detected directly in liquid scintillation detectors which, as well as retaining spectral information, means that thermalisation is not necessary. This reduces the amount of heavy, cumbersome material required as part of the fabric of a detector array; the detectors are also portable and modular, so they can be used in various arrangements without the need for moderator materials [19]. Gross γ-ray information, although not affording spectroscopy, can also be collected concurrently with the neutron data, unlike ^{3}He detectors. It is worthy of note that a great deal of operational experience exists associated with the use of ^{3}He and detector systems based on this have the intrinsic benefits of long-term stability and immunity to γ-ray interference.

2. Method

The measurements described in this research were carried out in the Engineering Department at Lancaster University, UK. The detection equipment consisted of four organic scintillation detectors of type VS-1105-21 (Scionix, Netherlands) containing EJ-309 scintillant (Eljen Technology, Sweetwater, TX) [20], a 4-channel Mixed Field Analyser, model MFAX4.3 (MFA, Hybrid Instruments Ltd., U.K.) [21], a custom data acquisition module [22] and a conventional laptop

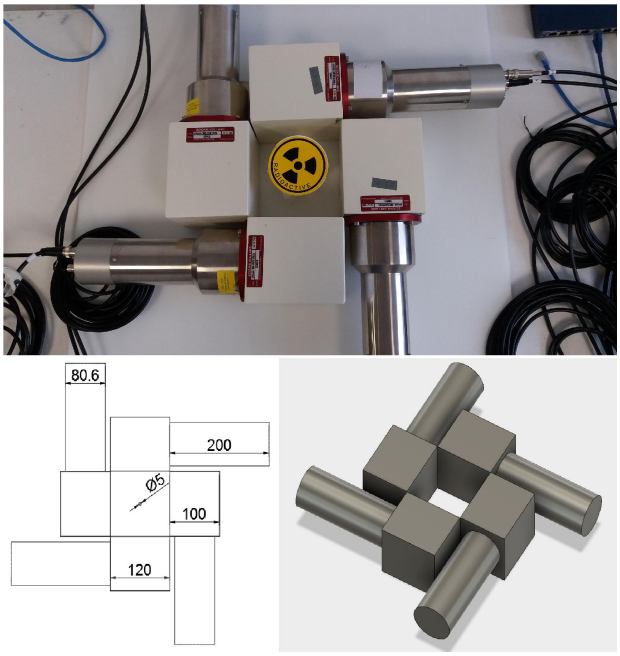

Figure 2: A photograph and drawings of the detector array used for the assessment of spontaneous fission neutrons from 0.3% wt. DUO_2 in this research. The dimensions stated here (in mm) were used for simulating the detector set-up in MCNP-6.

computer. Each measurement was performed for 18 hours. The detectors were placed in an orthogonal arrangement around a central void in which the samples were placed, as shown in Fig. 2. The four EJ-309 organic scintillation detectors were sandwiched between two layers of 10-mm thickness, high-density polyethylene, which reduced the influence of ambient background, particularly that from cosmic sources, the reduction was measured to be 1.48%. A background measurement was also employed to correct for ambient and cosmic sources of radiation. The background measurement was taken over the same period of the 24 hour clock as the experiments, to remove contributions by the diurnal effect on background, the greatest contributor to background radiation variation [23]. Cosmically-induced fissions were considered; comparing the volume of the detectors used (1200 cm^3) to the volume of the samples used (0.38 - 1.50 cm^3), the detectors have a volume that is a factor of 3.2×10^{-4} - 12.5×10^{-4} greater. Given that in lead (Pb), a suitable surrogate in this case for DUO_2, a cosmic flux produces a ratio of outgoing neutrons to incoming neutrons of 2.4 [24], our samples produce 7.68×10^{-4} - 30.0×10^{-4} neutrons per neutron detected directly from cosmic events. With the rates being this low, they were neglected for the measurements taken here, however, if larger samples or materials with greater fissionable mass were to be measured using this technique, this calculation would not stand and the new samples would need to be re-considered with respect to cosmically-induced fission.

Due to the close proximity of the four detectors, the effect of inter-detector scattering (cross-talk between detectors) was investigated experimentally and in MCNP-6 [25]. The data from a single detector were compared to a four-detector array in order to quantify the number of extra neutrons observed with the four-detector array as a result. However, the neutron count (per

detector) was consistently higher for the single detector arrangement, by approximately 25%. It is proposed that the increase in hydrogenous material from one to four detectors moderates neutrons within the geometry and down-scatters them below the detector threshold at approximately 0.5 MeV [26]. This spectrum softening was tested in two MCNP-6 models, one with an array of four detectors and one with just one detector, the results of which can be seen in Fig. 3. The model measured the neutron flux in one detector when on its own, and when in a four-detector array, the results of which passed all inherent MCNP statistical tests and had acceptable fractional standard deviations in line with [27]. The neutron flux below 0.5 MeV was shown to be greater in the four-detector array, and above 0.5 MeV the neutron flux was greater in the single-detector, thus the softening of the spectrum was shown to be plausible; an intrinsic influence of the measuring system on the field as measured. The mean flux was calculated to be 11.35% higher for the single detector alone, than when in a four-detector arrangement, broadly in agreement with the 25% measured experimentally. The difference between these two results could be attributed to bleedthrough in the PSD at low energies, where neutrons and γ rays can be confused. In contrast MCNP-6 does not have this issue, and reports definitive numbers of neutrons and γ rays. There have been multiple papers published providing correction factors for cross-talk measurements [28, 29, 30, 31]. Our sample emission rates were deemed too low to be able to confidently, statistically correct for the scattered neutrons. For the purposes of this experiment, the measured factor of 25% and the simulated factor of 11.35% imply that the effects of scatter are not a significant source of over-response for our four-detector array, but in fact depressing the number of counts measured here. Self shielding within the samples was not investigated due to the small volumes of the samples used. These scattering results open a debate as to whether increasing the solid angle of detector coverage is outweighed by the spectrum softening that will occur, when trying to increase detection efficiency of systems similar to that used here.

The detectors were calibrated via the MFA software operated in pulse gradient analysis (PGA) mode and with a ^{137}Cs source to obtain consistent response functions across all four detectors [32]. The Compton edges of each detector were aligned and a suitable neutron/γ-ray pulse-shape discrimination (PSD) threshold was applied. Once calibrated, the neutron and γ-ray TTL outputs from the MFA were connected to a data counter and a measurement of background radiation was carried out, comprising the detector array with no sample present. The latter was subtracted from the results obtained after assessing the DUO_2 samples in order to give the background-corrected radiation count for each sample. Following the background count, each DUO_2 sample was assessed in turn. Details of the samples used in this research are given in Table 4 along with predicted neutron emission rates for each sample. The DUO_2 was used in the form of slices of a depleted uranium pellet, each of mass up to 2 g. These pellet slices were combined to constitute the masses used during these assays. The pellets were stored inside air-tight plastic bags which were placed inside a plastic box.

The data counter was used in a logging mode to sum the number of neutron and γ-ray counts produced by each detector at intervals of approximately 1.15 s. The total number of neutrons and γ rays counted in each detector were then recorded. Each measurement resulted in eight pieces of information: the neutron and γ-ray count for each of the four detectors. Systematic errors were reduced by the use of a logging function rather than a real-time counter as this allowed for analysis of the second-by-second data. This was used to confirm that the detected radiation exhibited a Poisson distribution. The logging function also enabled the stability of the electronics to be checked periodically.

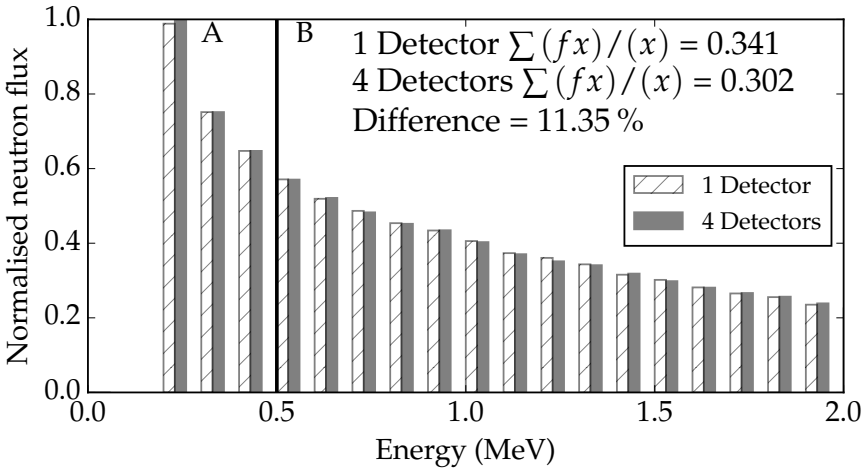

Figure 3: Results from an MCNP-6 model showing a spectral softening of the neutron flux in the same detector when four detectors are present in comparison to just one detector. This validates the experimental test which concluded that scattering of neutrons within the four-detector array was not increasing the number of neutrons detected per detector, but reducing them, due to the EJ-309 detectors having low efficiencies at low neutron energies. The neutron flux below 0.5 MeV was shown to be greater in the four-detector array, and above 0.5 MeV the neutron flux was greater in the single-detector. The mean neutron flux across the range of energy 0-10 MeV was calculated to be 11.35% higher for the same detector alone, than within a four-detector array. At 0.7 MeV the single detector overtakes the efficiency of the same detector in a four-detector array.

Mass UO_2 (g)	Mass of ^{238}U (g)	Predicted SF neutron emission (n s^{-1})	Predicted (α, n) neutron emission (n s^{-1})
4.20	3.69	0.050	3.69×10^{-4}
7.97	7.00	0.095	7.00×10^{-4}
12.25	10.77	0.146	10.77×10^{-4}
16.45	14.46	0.197	14.46×10^{-4}

Table 4: Details of 0.3 % wt. DUO_2 samples assessed in this research, along with associated spontaneous fission (SF) and alpha-n (α, n) predicted emission rates.

Mass UO_2 (g)	Mass of ^{238}U (g)	Net Neutron Count	Net Neutron CPS	Net γ-ray Count /$\times 10^7$	Net γ-ray CPS
4.20	3.69	274 ± 83	0.004 ± 0.001	1.71 ± 0.04%	264.6 ± 0.1
7.97	7.00	333 ± 84	0.005 ± 0.001	3.01 ± 0.03%	464.0 ± 0.1
12.25	10.77	591 ± 85	0.009 ± 0.001	4.73 ± 0.02%	730.7 ± 0.1
16.45	14.46	911 ± 87	0.014 ± 0.001	6.55 ± 0.02%	1011.2 ± 0.2

Table 5: Net counts of neutron and γ rays during 18-hour passive assessments as a function of DUO_2 mass. Errors were propagated from a square root of the background and the measured values.

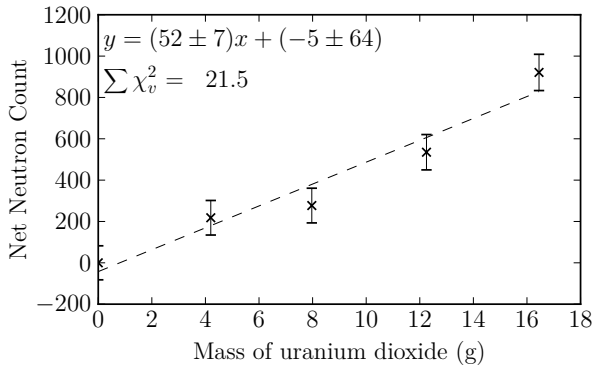

Figure 4: Net number of neutron counts summed over four detectors from the assay of various masses of 0.3% wt. depleted uranium dioxide over 18 hours (a line of best fit, errors of 1σ and reduced chi-squared are included; where x equals the mass of uranium dioxide (g) and y equals the net neutron counts).

3. Results

The results of the four measurements are presented as *net* results when background components are subtracted from the gross counts, and the results in Table 5 are obtained. Errors associated with each measurement have been propagated using the square root of both the background count and the measured values. The relatively high ratio or error for the net neutron count is an artefact of the large background count measured due to the prolonged measurement time. This time period was necessary due to the low neutron emission rate from the sample.

The net results are also presented in graphical form to allow for easier interpretation. Figures 4 and 5 show the net neutron count and net γ-ray count respectively. From the graphs presented throughout, the lines-of-best-fit and ${\chi_\nu}^2$ values have been collated and are presented in Table 6. This table also presents fit parameters for equations of lines that describe the sensitivity of the approach used here. This information has been calculated by normalising the data collected in terms of counts per second, per detector, per gram of DUO_2.

4. Analysis

The net neutron count from each of the samples studied in this research exhibits a positive trend with mass, with a line-of-best-fit equal to $y = (52 \pm 7)\ x + (-5 \pm 64)$; where x equals the

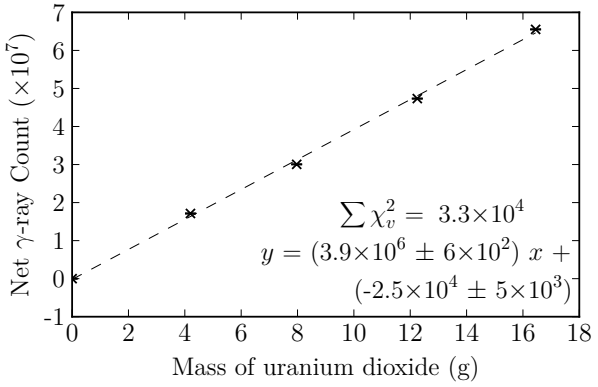

Figure 5: Net number of γ-ray counts summed over four detectors, from the assay of various masses of 0.3% wt. depleted uranium dioxide, over 18 hours (a line of best fit, errors of 1σ and reduced chi-squared are included; where x equals the mass of uranium dioxide (g) and y equals the net γ-ray counts). The size of the reduced chi-squared value is discussed in Section 4; the dashed line is used here to guide the reader's eye.

	CPS per detector per g (UO_2)				
	Form of equation of line: $y = (m \pm \Delta m)x + (c \pm \Delta c)$				
Result type	m	Δ m	c	Δ c	$\chi_\nu{}^2$
Net neutron: Fig. 4	2.01×10^{-04}	3×10^{-05}	-2.05×10^{-05}	2×10^{-04}	8.0×10^{-05}
Net γ ray: Fig. 5	$1.51\times10^{+01}$	2×10^{-03}	-9.65×10^{-02}	2×10^{-02}	0.128

Table 6: Fit parameters for the results obtained in Table 5. The table is split into two sections, giving fit parameters for different shapes of fit-line as described above each section, normalised to their Counts Per Second (CPS) per detector per gram of DUO_2. $\chi_\nu{}^2$ values for each line-of-fit are also included, the large values are discussed and analysed in section 4.

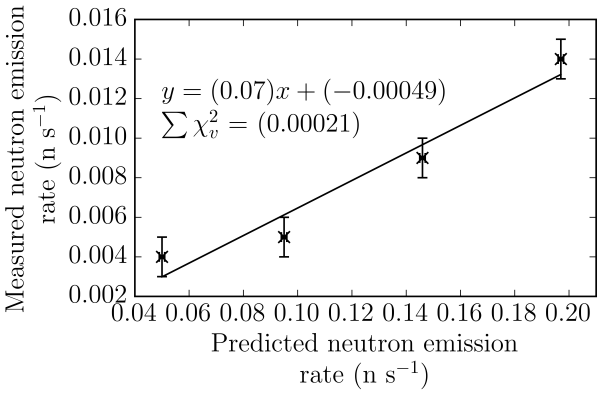

Figure 6: Predicted and measured neutron emission and detection rates at various masses of 0.3% wt. depleted uranium dioxide (errors of 1 standard deviation, a line of best fit, and reduced chi-squared are included; where x equals the predicted neutron emission rate from Table 4 (n s^{-1}) and y equals the measured neutron count rate from Table 5 (n s^{-1})).

mass of uranium dioxide (g) and y equals the net neutron count. As stated earlier, PSD allows discriminationof neutrons and γ rays. The net γ-ray count also shows a positive trend, with a line of best fit equal to $y = (3.9 \times 10^6 \pm 6 \times 10^2)\ x + (-2.4 \times 10^4 \pm 5 \times 10^3)$; where x equals the mass of uranium dioxide (g) and y equals the net γ-ray count.

Plotting the predicted neutron emission rate of each sample against the measured neutron count rate produces Fig. 6. This positive correlation gives an absolute efficiency of the detector system of ~7%. Given that the solid angle of the detector system is roughly 2/3 of 4-π space (four sides of a cube around the samples are comprised of detector material), the average energy of a ^{238}U spontaneous fission neutron is 0.8 MeV [33], and EJ-309 detection efficiency at this energy is ~20% with a 0.1 MeVee threshold [26], we would expect an average absolute efficiency in the region of 13.3%. This average absolute efficiency ignores errors with each of these measurements (predicted neutron emission rate, measured neutron rate, efficiency of detector system, and average neutron energy emitted) that would require intensive computational effort to convolute and combine, for little benefit. The simplistic predicted efficiency of the system also fails to take into account errors associated with using PSD techniques, particularly at low neutron energies, self-shielding, and induced fission neutron energies. With this knowledge of the inadequacies of our predicted efficiency, we believe our measured 7% efficiency and the predicted 13% efficiency are suitably similar.

There are limited comparisons to be drawn between this method and previous reports due to the low fission neutron emission rate of ^{238}U, resulting in there being relatively little investigation of its potential for uranium assessment. Research into the detection of neutron emissions from the spontaneous fission of ^{238}U has focussed predominantly on measuring the decay constant [34, 35, 36, 37]. An ionization chamber has been used for similar studies using low-mass, heavy-element samples [38]. In that report, 2800 events of ^{238}U spontaneous fission were measured, at a similar count rate. However, the applications of such technology are not readily comparable with the methods discussed here. Most ionisation chambers are stationary and have samples brought to them. Whilst portable ionisation chambers exist, they have much lower efficiencies than the detector system described here. It is feasible for the system described in this paper to be packed up and transported onto nuclear sites for the passive assessment of materials, in-situ.

Goddard and Croft [39] assayed U_3O_8 passively, concluding that nuclear data available at that time was insufficient to create useful models of the reactions. The paper focused on multiplicity measurements and aligns with the work in this paper with regards to the SF and (α, n) reaction rates. Of the neutron-singles data presented, the research suggests that MCNPX models align well with measured data, although there is negative trend in the ratio as enrichment increases [39, Fig. 8]. At 0.3% wt. enrichment, as utilised in the work carried out for this paper, there are no data, and the closest point to this has a ratio of ~1.022 between the measured and MCNPX values. This suggests that the MCNP-6 model used in this work is reliable. There are inconsistencies between the research presented here, and [39, Fig. 11] with respect to the declared singles count rate efficiencies. Goddard and Croft [39] states that efficiencies for SF neutrons are between 66.5% and 67.0% for all enrichments of U_3O_8, and we declare efficiency of ~7%. However the detection systems are different, and [39] uses the Los Alamos Epithermal Neutron Multiplicity Counter (ENMC). The ENMC is constructed of ^{3}He tubes which detect neutrons across the whole spectrum of energies. It would be expected that the ENMC would have a much greater efficiency than the EJ-309 detectors utilised in this research given the spectrum of SF neutrons from ^{238}U [33].

The PSD data produced during each of the assessments that comprise this experiment were plotted to ensure that the neutron and γ-ray plumes were as expected. Each of the five assays contained patches of noise above the γ-ray plume, as presented in Fig. 7. It is expected that these patches of noise are an artefact of running the assessments for long periods of time, and the effects of the noise can be seen clearly in the chi-squared values for the net-γ-ray count (Fig. 5). As all the noise artefacts (*clouds*) are manifested above the neutron/γ-ray threshold, in the γ-ray region, the neutron data presented here are considered to be sound and unaffected by this effect. Calculations show that these clouds account for less than 0.16% of the radiation events counted here. Further research is under way to identify the origin of this noise and eliminate the clouds alltogether.

In order to quantify the proportion of neutrons from the (α, n) reaction, a *SOURCES* simulation of this particular sample was conducted [40]. The neutron production rate of 0.3% wt. DUO_2 is given as 7.17×10^{-5} n g^{-1} s^{-1}. This rate of neutron production is a factor of ~189 less than the neutron production rate of spontaneous neutrons from ^{238}U, and so, when considering the results it is reasonable to consider the neutron flux from the (α, n) reaction as negligible relative to that from spontaneous fission.

5. Future Work

Although the erroneous noise patches in the γ-region of the PSD data have been quantified here, the source of these patches should be identified. If the system were to be considered for measuring greater quantities of SNM, methods would need to be devised to correct for neutron multiplication effects, cosmically-induced fission, α, n contributions, and isotopics of the sample. This would not be an insignificant task.

6. Conclusion

The ability to detect neutrons using organic liquid scintillation detectors passively, predominantly from the spontaneous fission of ^{238}U in uranium dioxide has been demonstrated. Masses of ^{238}U between 3.69 g and 14.46 g have been assessed over 18-hour periods. This method has

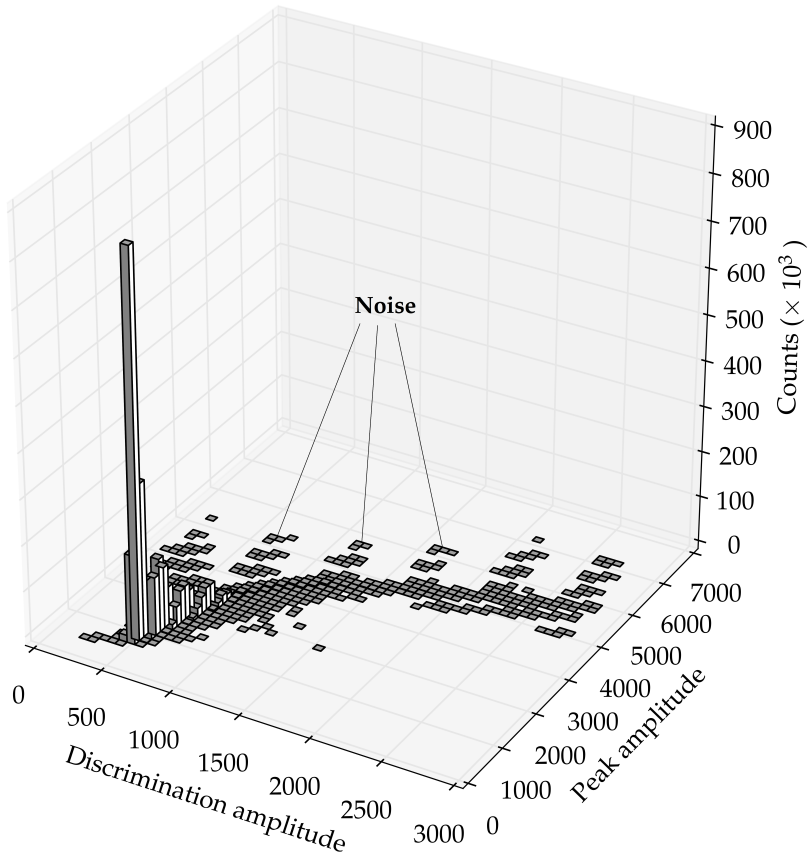

Figure 7: A histogram of PSD data from long term measurement (46 hours) of background radiation showing *clouds* of noise in the γ-ray region. No neutron/γ-ray threshold is plotted as no neutron source was present.

potential applications in the nuclear industry in scenarios associated with radioactive waste assay, total uranium assessment of ores, tails monitoring, environmental assessment and in forensic analysis. The method utilises four EJ-309 detectors and could be scaled up easily on a modular basis to assess larger quantities of ^{238}U-containing material. The method presented here also shows promise for measuring total uranium content of bulk quantities of substance. At present, this method is presented as a proof of concept with an emphasis on the passive measurement of very low neutron emission rates. Further work would be required to bring the method up to technical readiness if it were to be deployed in real life scenarios.

Acknowledgement

The authors would like to acknowledge the UK Engineering and Physical Sciences Research Council under grants DISTINCTIVE EP/L014041/1 and ADRIANA EP/L025671/1, the latter as part of the UK National Nuclear User Facility, Lee Packer at CCFE, for the results of the *SOURCES* simulation into the (α, n) reaction rate of 0.3% wt. DUO_2, and Zoltan Hielz at Imperial College London and NNL at Springfields for the production of the depleted uranium dioxide pellets. Malcolm J. Joyce acknowledges the receipt of a Royal Society Wolfson Research Merit Award.

[1] E. Craft, A. Abu-Qare, M. Flaherty, M. Garofolo, H. Rincavage, M. Abou-Donia, Depleted and natural uranium: chemistry and toxicological effects, Journal of Toxicology and Environmental Health. Part B, Critical Reviews 7 (4) (2004) 297–317. doi:10.1080/10937400490452714.

[2] S. A. Katz, The Chemistry and Toxicology of Depleted Uranium, Toxics 2 (1) (2014) 50–78. doi:10.3390/toxics2010050.
URL http://www.mdpi.com/2305-6304/2/1/50

[3] A. Bleise, P. R. Danesi, W. Burkart, Properties, use and health effects of depleted uranium (DU): a general overview, Journal of Environmental Radioactivity 64 (2-3) (2003) 93–112.

[4] W. E. Briner, The evolution of depleted uranium as an environmental risk factor: lessons from other metals, International Journal of Environmental Research and Public Health 3 (2) (2006) 129–135.

[5] WNTI, Fact Sheet - Uranium Hexaflouride, Tech. rep., World Nuclear Transport Institute, London, U.K.
URL http://www.wnti.co.uk/media/76713/WNTI%20-%20FS%20UF6%20-%20FINAL%20FINAL%205%208%2015%20-JK%20approved.pdf

[6] D. Reilly, N. Ensslin, J. Hastings Smith, S. Kreiner, Passive nondestructive assay of nuclear materials PANDA, United States Nuclear Regulatory Commission, Los Alamos National Laboratory, 1993.

[7] Global Threat Reduction Programme: Nuclear Security Programme - Case study - GOV.UK (Jan. 2013).
URL https://www.gov.uk/government/case-studies/global-threat-reduction-programme-nuclear-security-programme

[8] IAEA, Preparing for Future Verification Challenges.
URL http://www-pub.iaea.org/books/IAEABooks/8857/Preparing-for-Future-Verification-Challenges

[9] D. Senior, Guidance on the Demonstration of ALARP (As Low As Reasonably Practicable), Guide NS-TAST-GD-005 Revision 7, Office for Nuclear Regulation (Dec. 2015).
URL http://www.onr.org.uk/operational/tech_asst_guides/ns-tast-gd-005.pdf

[10] R. Vogt, J. Randrup, Event-by-event study of neutron observables in spontaneous and thermal fission, Physical Review C 84 (4) (2011) 044621. doi:10.1103/PhysRevC.84.044621.
URL https://link.aps.org/doi/10.1103/PhysRevC.84.044621

[11] H. J. Ahmed, J. L. Fogg, Method and apparatus for passively gamma scanning a nuclear fuel rod (Sep. 1988).
URL https://patents.google.com/patent/EP0280925A1/en

[12] M. H. Khan, P. Warwick, N. Evans, Spectrophotometric determination of uranium with arsenazo-III in perchloric acid, Chemosphere 63 (7) (2006) 1165–1169. doi:10.1016/j.chemosphere.2005.09.060.
URL http://www.sciencedirect.com/science/article/pii/S0045653505011513

[13] T. Gozani, Active Nondestructive Assay of Nuclear Materials: Principles and Applications, Tech. Rep. NUREG/CR-0602; SAI-MLM-2585, Science Applications, Inc., Palo Alto, CA (USA); Monsanto Research Corp.,

Miamisburg, OH (USA). Mound (Jan. 1981).
URL http://www.osti.gov/scitech/biblio/6215952

[14] G. A. Wagner, G. M. Reimer, B. S. Carpenter, H. Faul, R. Van Der Linden, R. Gijbels, The spontaneous fission rate of U-238 and fission track dating, Geochimica et Cosmochimica Acta 39 (9) (1975) 1279–1286. doi:10.1016/0016-7037(75)90135-0.
URL http://www.sciencedirect.com/science/article/pii/0016703775901350

[15] G. F. Knoll, Radiation detection and measurement Glenn F. Knoll 3rd ed 1999.pdf, 1999.
URL https://ia600207.us.archive.org/22/items/RadiationDetectionAndMeasurementGlennF.Knoll3rdEd1999/Radiation%20detection%20and%20measurement%20Glenn%20F.%20Knoll%203rd%20ed%201999.pdf

[16] G. Hu, W. Kang, Y.-C. Xiang, Z.-H. Xiong, F.-H. Hao, H.-L. Wu, L. Cao, C.-F. Zhang, Mass measurement of depleted uranium components with coincidence neutron count, Yuanzineng Kexue Jishu/Atomic Energy Science and Technology 46 (7) (2012) 871–877.

[17] G. Knoll, Radiation Measurement - Passive detectors. Encyclopdia Britannica Online. (2016).
URL https://www.britannica.com/technology/radiation-measurement/Passive-detectors#ref620737

[18] A. Enqvist, C. C. Lawrence, B. M. Wieger, S. A. Pozzi, T. N. Massey, Neutron light output response and resolution functions in EJ-309 liquid scintillation detectors, Nuclear Instruments and Methods in Physics Research Section A: Accelerators, Spectrometers, Detectors and Associated Equipment 715 (2013) 79–86. doi:10.1016/j.nima.2013.03.032.
URL http://www.sciencedirect.com/science/article/pii/S0168900213003203

[19] H. M. O. Parker, M. D. Aspinall, A. Couture, F. D. Cave, C. Orr, B. Swinson, M. J. Joyce, Active fast neutron singles assay of 235u enrichment in small samples of triuranium octoxide, Progress in Nuclear Energy 93 (2016) 59–66. doi:10.1016/j.pnucene.2016.07.022.
URL http://www.sciencedirect.com/science/article/pii/S0149197016301688

[20] A. Tomanin, J. Paepen, P. Schillebeeckx, R. Wynants, R. Nolte, A. Lavietes, Characterization of a cubic EJ-309 liquid scintillator detector, Nuclear Instruments and Methods in Physics Research Section A: Accelerators, Spectrometers, Detectors and Associated Equipment 756 (2014) 45–54. doi:10.1016/j.nima.2014.03.028.
URL http://www.sciencedirect.com/science/article/pii/S0168900214003222

[21] A. Lavietes, R. Plenteda, N. Mascarenhas, L. M. Cronholm, M. Aspinall, M. Joyce, A. Tomanin, P. Peerani, Development of a liquid scintillator-based active interrogation system for LEU fuel assemblies, in: 2013 3rd International Conference on Advancements in Nuclear Instrumentation, Measurement Methods and their Applications (ANIMMA), 2013, pp. 1–4. doi:10.1109/ANIMMA.2013.6728037.

[22] J. Beaumont, Characterisation of radiation fields with combined fast-neutron and gamma-ray imaging, Tech. rep., dOI: 10.17635/lancaster/thesis/33 (2017).
URL http://www.research.lancs.ac.uk/portal/en/publications/characterisation-of-radiation-fields-with-combined-fastneutron-and-gammaray-imaging(253967f6-7029-4b67-b983-9a33ae89b77b).html

[23] A. Simpson, M. Clapham, Methods for Reduction of the Minimal Detectable Activity in Neutron Assay of High Mass/High Z Objects.pdf, Phoenix, Arizona, USA, 2014.
URL http://www.wmsym.org/archives/2014/papers/14504.pdf

[24] E. Aguayo, R. T. Kouzes, E. R. Siciliano, Neutron spallation measurements and impacts on low-background experiments, Physical Review C 90 (3). doi:10.1103/PhysRevC.90.034607.
URL https://link.aps.org/doi/10.1103/PhysRevC.90.034607

[25] T. Goorley, e. al., Initial MCNP6 release Overview (Dec. 2012).

[26] F. Pino, L. Stevanato, D. Cester, G. Nebbia, L. Sajo-Bohus, G. Viesti, The light output and the detection efficiency of the liquid scintillator EJ-309, Applied Radiation and Isotopes: Including Data, Instrumentation and Methods for Use in Agriculture, Industry and Medicine 89 (2014) 79–84. doi:10.1016/j.apradiso.2014.02.016.

[27] Hussein, Esam M. A., Monte Carlo Particle Transport with the MCNP Code, Tech. rep., University of New Brunswick, Canada, Department of Mechanical Engineering.
URL https://canteach.candu.org/Content%20Library/20043524.pdf

[28] J. Wang, A. Galonsky, J. J. Kruse, P. D. Zecher, F. Dek, . Horvth, . Kiss, Z. Seres, K. Ieki, Y. Iwata, Neutron cross-talk in a multi-detector system, Nuclear Instruments and Methods in Physics Research Section A: Accelerators, Spectrometers, Detectors and Associated Equipment 397 (2) (1997) 380–390. doi:10.1016/S0168-9002(97)00806-1.
URL http://www.sciencedirect.com/science/article/pii/S0168900297008061

[29] F. M. Marqus, M. Labiche, N. A. Orr, F. Sarazin, J. C. Anglique, Neutron cross-talk rejection in a modular array and the detection of halo neutrons, Nuclear Instruments and Methods in Physics Research Section A: Accelerators, Spectrometers, Detectors and Associated Equipment 450 (1) (2000) 109–118. doi:10.1016/S0168-9002(00)

00248-5.
URL http://www.sciencedirect.com/science/article/pii/S0168900200002485

[30] T. H. Shin, M. J. Marcath, A. DiFulvio, S. D. Clarke, S. A. Pozzi, Neutron cross-talk characterization of liquid organic scintillators, in: 2015 IEEE Nuclear Science Symposium and Medical Imaging Conference (NSS/MIC), 2015, pp. 1–4. doi:10.1109/NSSMIC.2015.7581911.

[31] J. Verbeke, M. Prasad, N. Snyderman, Neutron crosstalk between liquid scintillators, Nuclear Instruments and Methods in Physics Research Section A: Accelerators, Spectrometers, Detectors and Associated Equipment 794 (2015) 127–140. doi:10.1016/j.nima.2015.04.019.
URL http://linkinghub.elsevier.com/retrieve/pii/S0168900215004921

[32] B. DMellow, M. Aspinall, R. Mackin, M. Joyce, A. Peyton, Digital discrimination of neutrons and -rays in liquid scintillators using pulse gradient analysis, Nuclear Instruments and Methods in Physics Research Section A: Accelerators, Spectrometers, Detectors and Associated Equipment 578 (1) (2007) 191–197. doi:10.1016/j.nima.2007.04.174.
URL http://www.sciencedirect.com/science/article/pii/S0168900207008194

[33] A. Alexandrov, T. Asada, A. Buonaura, L. Consiglio, N. DAmbrosio, G. De Lellis, A. Di Crescenzo, N. Di Marco, M. Di Vacri, S. Furuya, G. Galati, V. Gentile, T. Katsuragawa, M. Laubenstein, A. Lauria, P. Loverre, S. Machii, P. Monacelli, M. Montesi, T. Naka, F. Pupilli, G. Rosa, O. Sato, P. Strolin, V. Tioukov, A. Umemoto, M. Yoshimoto, Intrinsic neutron background of nuclear emulsions for directional Dark Matter searches, Astroparticle Physics 80 (2016) 16–21. doi:10.1016/j.astropartphys.2016.03.003.
URL http://linkinghub.elsevier.com/retrieve/pii/S0927650516300354

[34] J. H. Roberts, R. Gold, R. J. Armani, Spontaneous-Fission Decay Constant of 238u, Physical Review 174 (1968) 1482–1484. doi:10.1103/PhysRev.174.1482.
URL http://adsabs.harvard.edu/abs/1968PhRv..174.1482R

[35] A. G. Popeko, G. M. Ter-Akopian, Measurement of the 238u spontaneous-fission halflife by detecting prompt neutrons, Nuclear Instruments and Methods 178 (1) (1980) 163–165. doi:10.1016/0029-554X(80)90871-X.
URL http://www.sciencedirect.com/science/article/pii/0029554X8090871X

[36] S. Guedes, J. C. N. Hadler, J. E. S. Sarkis, K. M. G. Oliveira, M. H. Kakazu, P. J. Iunes, M. Saiki, C. a. S. Tello, S. R. Paulo, Spontaneous-fission decay constant of 238u measured by nuclear track techniques without neutron irradiation, Journal of Radioanalytical and Nuclear Chemistry 258 (1) (2003) 117–122. doi:10.1023/A:1026218411554.
URL https://link.springer.com/article/10.1023/A:1026218411554

[37] T. Yoshioka, T. Tsuruta, H. Iwano, T. Danhara, Spontaneous fission decay constant of 238u determined by SSNTD method using CR-39 and DAP plates, Nuclear Instruments and Methods in Physics Research Section A: Accelerators, Spectrometers, Detectors and Associated Equipment 555 (12) (2005) 386–395. doi:10.1016/j.nima.2005.09.014.
URL http://www.sciencedirect.com/science/article/pii/S0168900205018243

[38] M. P. Ivanov, G. M. Ter-Akopian, B. V. Fefilov, A. S. Voronin, Study of 238u spontaneous fission using a double ionization chamber, Nuclear Instruments and Methods in Physics Research Section A: Accelerators, Spectrometers, Detectors and Associated Equipment 234 (1) (1985) 152–157. doi:10.1016/0168-9002(85)90821-6.
URL http://www.sciencedirect.com/science/article/pii/0168900285908216

[39] B. Goddard, S. Croft, High-fidelity passive neutron multiplicity measurements and simulations of uranium oxide, Nuclear Instruments and Methods in Physics Research Section A: Accelerators, Spectrometers, Detectors and Associated Equipment 712 (2013) 147–156. doi:10.1016/j.nima.2013.02.007.
URL http://www.sciencedirect.com/science/article/pii/S0168900213001836

[40] LANL, SOURCES-4c: Code System For Calculating alpha,n; Spontaneous Fission; and Delayed Neutron Sources and Spectra. (Jul. 2002).
URL https://rsicc.ornl.gov/codes/ccc/ccc6/ccc-661.html